

Beamformed Radio Link Capacity under Positioning Uncertainty

Jukka Talvitie, *Member, IEEE*, Toni Levanen, *Member, IEEE*, Mike Koivisto, *Student Member, IEEE*, Tero Ihalainen, Kari Pajukoski, and Mikko Valkama, *Senior Member, IEEE*

Abstract—Beamforming is one of the key technologies for achieving the high performance criteria in various modern and future wireless communications systems, in particular at the millimeter wave frequencies. In order to avoid or reduce the large signaling overhead and corresponding latency related to beam-training procedures, location-based beamforming utilizing available position information has been proposed. In this paper, by using the available position probability density function of a receiving device, we derive and analyze the capacity of a beamformed radio link, without and with beam-sweeping based beam training. Through the analysis, we show that by adjusting the beamforming and/or beam-training parameters appropriately, the radio link capacity can be optimized with respect to the prevailing positioning accuracy, and thus optimal utilization of radio resources is achieved with minimal radio access latency.

Index Terms—channel capacity, mmWave, beamforming, beam-training, positioning, wireless networks, location-awareness

I. INTRODUCTION

Various modern and emerging wireless communications systems, such as the fifth generation (5G) and beyond mobile networks, support operation at the so-called millimeter wave (mmWave) bands, where the scarcity of the spectrum is significantly alleviated [1]–[3]. In order to compensate for the increased propagation losses at higher frequencies, multiple-input multiple-output (MIMO) antenna systems with beamforming capability are an essential technology to fulfill the demanding performance criteria [4]. The small wavelength at mmWaves enables the use of high-resolution beamforming via massive antenna arrays, where a large number of antenna elements can be packed into small area or volume.

Although accurate beamforming has a great potential to improve the performance of wireless systems, there are significant challenges that must be considered in order to reveal the full potential of the considered technology. From the communications system and radio protocols perspective, one of the greatest challenges is the beam management, where the fundamental target is to establish and maintain a beam pair between the transmitter (TX) and receiver (RX) in such a way that certain desired performance indicators are optimized. However, as shown in [5]–[8], training and tracking of beams can consume a lot of valuable channel resources which increases the training overhead, and thus reduces the capacity of the system. Additionally, demanding beam-training procedures increase the channel access latency.

In order to reduce the beam-training overhead, location-aware communications, and especially location-based beamforming, have been proposed and discussed, e.g., in [9]–[11]. There, the fundamental idea is to utilize the estimated device position for aligning the transmit and receive beams. However, the effect of the positioning error, or generally the underlying uncertainty of the available position information, has not been considered in the existing literature, particularly in configuring the beamforming parameters. Furthermore, as shown in [7], [12], there is an evident trade-off between the positioning quality and the achieved data rate over a beamformed communications link, however, no explicit capacity analysis including location uncertainty has been reported.

In this paper, instead of focusing on location-based beamforming relying on a single position estimate, we consider the available position probability density function (PDF). To this end, the main contribution of this article comprises novel derivations and analysis of a beamformed radio link capacity assuming the availability of an arbitrary position PDF, which can in practice be obtained, e.g., via Bayesian-based positioning and tracking algorithms [13], [14]. As shown by the provided numerical evaluations, the link capacity can be optimized with respect to the available position PDF for a certain number of used antenna elements, i.e., the beamwidth of the considered beamformer. In addition, it is shown that when explicit beam-sweeping based beam-training is used, an optimal number of trained beams can be found in terms of channel capacity. These are findings that have not been reported in the existing literature. Overall, the proposed novel approach enables improved efficiency in the utilization of radio resources, while also allowing for reduced channel access latency, as the beam-training related latency is reduced.

II. SYSTEM MODEL

A. Basic Assumptions and Received Signal Model

We consider a system model with a single TX at position $\mathbf{x}_T = [x_T, y_T]^T$, and a single RX at position $\mathbf{x} = [x, y]^T$, where x_T and x are the x-coordinates of the TX and RX, respectively, and y_T and y are the y-coordinates of the TX and RX, respectively. Both the TX and the RX are assumed to adopt a uniform linear array (ULA), capable of analog/RF beamforming. The considered system model builds on line-of-sight (LoS) based radio propagation assumption. However, the proposed approach can be further generalized to non-line-of-sight (NLoS) scenarios by utilizing PDFs of scatterer positions, as obtained, e.g., in [14]. In this specific framework, estimation of angle of departure (AoD) and angle of arrival (AoA) has a

J. Talvitie, T. Levanen, M. Koivisto, and M. Valkama are with Tampere University, Finland (firstname.lastname@tuni.fi).

T. Ihalainen and K. Pajukoski are with Nokia Bell Labs, Finland (firstname.lastname@nokia-bell-labs.com).

This manuscript contains [multimedia material](#).

key role in obtaining the scatterer position PDFs, which are required in the desired channel capacity evaluations.

Building on above assumptions, and assuming N and M antenna elements in the TX and RX arrays, respectively, the received signal sample reads

$$z(\mathbf{x}) = \sqrt{P_T} \zeta(\mathbf{x}) \mathbf{f}_R^H \mathbf{a}_R(\phi_R(\mathbf{x})) \mathbf{a}_T^H(\phi_T(\mathbf{x})) \mathbf{f}_T q + \mathbf{f}_R^H \mathbf{n}, \quad (1)$$

where P_T is the transmit power in Watts, q denotes the transmitted sample with unit power, and $\zeta(\mathbf{x})$ is the propagation loss coefficient at position \mathbf{x} , including path loss, shadowing, and all other losses and gains in the channel. Moreover, $\mathbf{n} \in \mathbb{C}^M$ denotes RX noise, and $\mathbf{f}_T \in \mathbb{C}^N$ and $\mathbf{f}_R \in \mathbb{C}^M$ are the transmit and receive beamforming vectors, respectively. Additionally, the steering vector $\mathbf{a}_T(\phi_T(\mathbf{x})) \in \mathbb{C}^N$ reads

$$\mathbf{a}_T(\phi_T(\mathbf{x})) = [a_{T,0}, a_{T,1}, \dots, a_{T,N-1}]^T \quad (2)$$

where $a_{T,m} = e^{j2\pi m \beta \sin(\phi_T(\mathbf{x}))}$ and $\beta = d_{\text{ant}}/\lambda$ is the ratio between the antenna element spacing d_{ant} and the used carrier wavelength λ , while $\mathbf{a}_R(\phi_R(\mathbf{x})) \in \mathbb{C}^M$ is defined similarly. Furthermore, for the considered LoS path at the RX position \mathbf{x} , the AoD and the AoA are given as $\phi_T(\mathbf{x}) = \text{atan}_2(y - y_T, x - x_T)$ and $\phi_R = -\phi_T$, respectively, where $\text{atan}_2(\cdot)$ is the four-quadrant inverse tangent.

In this work, it is assumed that the TX position \mathbf{x}_T as well as the orientation of the TX and RX are perfectly known. The RX position is assumed to be unknown, but by utilizing appropriate positioning methods, the PDF of the RX position $p_{\mathbf{x}}(\mathbf{x})$ can be assumed to be available, as illustrated in Fig. 1. For example, Kalman filters and its various extensions, such as the extended Kalman filter (EKF) [13], discussed and demonstrated in Section IV, inherently provide the PDF during the estimation and tracking process. However, whereas EKF-based estimates are limited to Gaussian distributions, the proposed method allows using arbitrary distributions, e.g., obtained with particle filters or sampling-based techniques [14].

B. Rationale

In this paper, the information on the RX position is utilized for location-based geometric beamforming, where the optimal beam direction is found either purely in a location-based manner, without executing any explicit beam-training methods, or by utilizing beam-sweeping based beam-training but taking the location information into account to reduce the associated training overhead and latency. Besides only focusing on the optimal beam direction, the proposed approach considers the level of uncertainty included in the available position estimate. For instance, with highly concentrated position PDFs, narrow beams can be practically always aligned for achieving large beam gains, whereas with broadly distributed PDFs, narrow beams find their targets rarely. In Fig. 1, there is an illustration of optional transmit beams with different beamwidths directed towards the assumed RX position. Although the narrowest beam with $N = 32$ antenna elements has potentially the highest beam gain, it has also a significant probability to severely miss the RX when there is uncertainty about the RX location. Hence, there is an apparent trade-off between the beam gain and the radio link availability, or reliability, which together affect the expected link capacity.

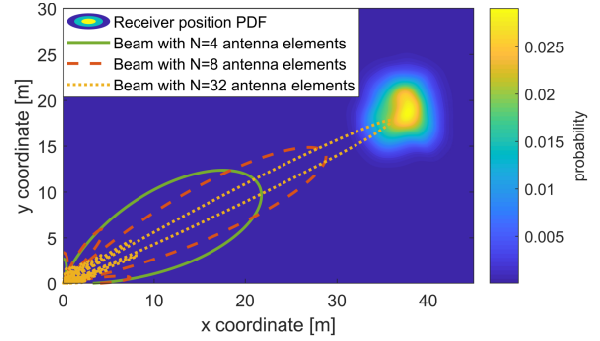


Fig. 1. Example illustration of receiver position PDF and optional transmit beams with various beamwidths, obtained by using different number of transmit antenna elements.

III. CHANNEL CAPACITY WITH POSITION INFORMATION

In this section, we derive and analyze the channel capacity for the beamformed radio link under the system model described in Section II. First, in Sub-section III-A, we consider a purely location-based beamforming system under the position uncertainty where no separate beam-training process takes place. Then, in Sub-section III-B, the corresponding capacity analysis is performed for the case with a dedicated beam-training process, where higher beam gains can potentially be achieved, while still leveraging the available position PDF to reduce the training overhead and latency.

A. Channel Capacity without Beam Training

According to the well-known Hartley-Shannon law, for given transmit beamformer \mathbf{f}_T and receive beamformer \mathbf{f}_R , the instantaneous channel capacity at an arbitrary RX position \mathbf{x} can be expressed as

$$C(\mathbf{x}, \mathbf{f}_T, \mathbf{f}_R) = \log_2 \left(1 + \frac{P_T |\zeta(\mathbf{x})|^2 \Phi(\mathbf{x}, \mathbf{f}_T, \mathbf{f}_R)}{\sigma_n^2} \right), \quad (3)$$

where

$$\Phi(\mathbf{x}, \mathbf{f}_T, \mathbf{f}_R) = |\mathbf{f}_T^H \mathbf{a}_T(\phi_T(\mathbf{x}))|^2 |\mathbf{f}_R^H \mathbf{a}_R(\phi_R(\mathbf{x}))|^2, \quad (4)$$

is the achieved beam gain, and σ_n^2 is the variance of noise after the receive beamformer. Moreover, it is assumed that the used transmit power P_T as well as the channel parameters $\zeta(\mathbf{x})$ and σ_n^2 are fixed, i.e., the capacity expression applies to given P_T , $\zeta(\mathbf{x})$ and σ_n^2 .

We assume a probabilistic RX position, expressed according to the position PDF $p_{\mathbf{x}}(\mathbf{x})$, which can be obtained, for example, by the EKF, as demonstrated in Section IV. Moreover, the cumulative distribution function of the capacity can be written as

$$F_C(\gamma) = \int_{\Psi} p_{\mathbf{x}}(\mathbf{x}) d^2\mathbf{x} = \int_0^{\gamma} p_C(\Lambda, \mathbf{f}_T, \mathbf{f}_R) d\Lambda \quad (5)$$

where $\Psi = \{\mathbf{x} \in \Omega \mid C(\mathbf{x}, \mathbf{f}_T, \mathbf{f}_R) \leq \gamma\}$, and $\Omega \subseteq \mathbb{R}^2$ is the set of possible RX positions with non-zero probability. Here, γ is a capacity value, which is used to collect all positions \mathbf{x} , where the capacity is less than or equal to γ , into the set Ψ . The corresponding PDF of the channel capacity can then be expressed as $p_C(\gamma, \mathbf{f}_T, \mathbf{f}_R) = \partial/\partial\gamma F_C(\gamma)$.

Although the above-described distributions are able to reveal the statistical behavior of the capacity through different system realizations, it is also useful to quantify the average capacity under the assumption of system ergodicity. Thus, based on (3), the expected value of the channel capacity can be written as

$$C_{\text{beam}} = E[C(\mathbf{x}, \mathbf{f}_T, \mathbf{f}_R)] = \int_{\mathbf{x} \in \Omega} C(\mathbf{x}, \mathbf{f}_T, \mathbf{f}_R) p_{\mathbf{x}}(\mathbf{x}) d^2 \mathbf{x} \quad (6)$$

$$= \int_{\mathbf{x} \in \Omega} \log_2 \left(1 + \frac{P_T |\zeta(\mathbf{x})|^2 \Phi(\mathbf{x}, \mathbf{f}_T, \mathbf{f}_R)}{\sigma_n^2} \right) p_{\mathbf{x}}(\mathbf{x}) d^2 \mathbf{x}, \quad (7)$$

which presents the ergodic channel capacity with the probabilistic RX position $p_{\mathbf{x}}(\mathbf{x})$ for given transmit and RX beamformers \mathbf{f}_T and \mathbf{f}_R , respectively.

B. Channel Capacity with Beam Training

Conventional beam-training methods rely on extensive beam-sweeping and measurement reporting procedures for finding the optimal transmit-receive beam-pairs. Compared to the scenario without beam training, discussed in Section III-A, beam training with position information enables utilization of narrower beams at the cost of beam training overhead. In beam-sweeping, different combinations of transmit and receive beams from the available beam set are tested while transmitting known reference signals. The trialed beam combinations can cover the whole beam set, or only a part of it – for example, by exploiting the position information or previously determined beam combinations. Moreover, the criterion for selecting the optimum beam pair is based on maximizing the received signal power corresponding to the received signal model given in (1). Under the assumption of noise-free beam measurements maximizing the received signal power also maximizes the achieved beamforming gain given in (4). Hence, we define the combination of optimal transmit and receive beams at RX position \mathbf{x} as

$$(\hat{k}, \hat{l}) = \arg \max_{k,l} \{ \Phi(\mathbf{x}, \tilde{\mathbf{f}}_T^{(k)}, \tilde{\mathbf{f}}_R^{(l)}) \} \quad (8)$$

where $\tilde{\mathbf{f}}_T^{(k)} \in \mathbb{C}^N$ is the beamforming vector related to the k^{th} transmit beam of the TX beam set, $\tilde{\mathbf{f}}_R^{(l)} \in \mathbb{C}^M$ is the beamforming vector related to the l^{th} receive beam of the RX beam set, and \hat{k} and \hat{l} are the indices for the optimal transmit and receive beams, respectively.

In order to define the channel capacity with beam training, the ergodic capacity given in (6) is utilized by dividing the integral into parts according to coverage areas of separate beams in the available beam set. Now, considering the full beam training through all available beams, the expected value of the channel capacity, deliberately excluding yet the training overhead, can be written as

$$\begin{aligned} \tilde{C}_{\text{train}} &= \sum_{k=0}^{K-1} \sum_{l=0}^{L-1} \int_{\mathbf{x} \in \Omega_{k,l}} C(\mathbf{x}, \tilde{\mathbf{f}}_T^{(k)}, \tilde{\mathbf{f}}_R^{(l)}) p_{\mathbf{x}}(\mathbf{x}) d^2 \mathbf{x} \\ &= \sum_{k=0}^{K-1} \sum_{l=0}^{L-1} \int_{\mathbf{x} \in \Omega_{k,l}} \log_2 \left(1 + \frac{P_T |\zeta(\mathbf{x})|^2 \Phi(\mathbf{x}, \tilde{\mathbf{f}}_T^{(k)}, \tilde{\mathbf{f}}_R^{(l)})}{\sigma_n^2} \right) p_{\mathbf{x}}(\mathbf{x}) d^2 \mathbf{x} \end{aligned} \quad (9)$$

where K and L are the total numbers of available beams in the beam sets of the TX and RX, respectively. Moreover, $\Omega_{k,l} \subseteq \Omega$ is the set of RX positions, where the maximum beam gain is achieved for the k^{th} transmit beam and l^{th} receive beam, defined as

$$\begin{aligned} \Omega_{k,l} &= \{ \mathbf{x} \in \Omega \mid \forall (k \neq m, l \neq n) \\ &\quad \Phi(\mathbf{x}, \tilde{\mathbf{f}}_T^{(k)}, \tilde{\mathbf{f}}_R^{(l)}) \geq \Phi(\mathbf{x}, \tilde{\mathbf{f}}_T^{(m)}, \tilde{\mathbf{f}}_R^{(n)}) \}, \end{aligned} \quad (10)$$

where in the case of equal beam gains, the designation to the appropriate set $\Omega_{k,l}$ can be based on beam index ordering, so that any position \mathbf{x} is included in only one set. We note that in low signal-to-noise ratio (SNR) conditions in real networks, there is a possibility of missing the optimum beam index. Thus, strictly-speaking, the above capacity expression represents an upper bound.

Next, by considering and utilizing the available position PDF, the training overhead can be reduced, compared to the full beam-sweeping, by considering training only for a subset of beams, which covers the area where the RX is most likely located. In this case, the beam training is performed in the order of position probability so that

$$\begin{aligned} P(\mathbf{x} \in \Omega_{k_1, l_1}) &\geq P(\mathbf{x} \in \Omega_{k_2, l_2}) \geq \dots \geq P(\mathbf{x} \in \Omega_{k_K, l_L}), \\ \text{with } P(\mathbf{x} \in \Omega_{k_i, l_i}) &= \int_{\mathbf{x} \in \Omega_{k_i, l_i}} p_{\mathbf{x}}(\mathbf{x}) d^2 \mathbf{x}, \end{aligned} \quad (11)$$

where k_i and l_i are the transmit and receive beam indices trained at the i^{th} turn. Now, by taking into account the required training overhead, the channel capacity with the beam training procedure becomes

$$C_{\text{train}} = (1 - \eta N_{\text{train}}) \tilde{C}_{\text{train}} \quad (12)$$

where N_{train} is the total number of trained beam combinations with $0 < \eta N_{\text{train}} \leq 1$, and $\eta \in (0, 1]$ is the training overhead, given as a ratio between the amount of radio resources used for training one beam pair and the amount all available radio resources in the considered transmission period.

C. Extension to Scenarios with Multiple Unknown Variables

In cases where the selection of the optimum transmit and receive beamforming vectors is affected by other unknown variables, besides the RX position, the capacity expression in (7) can be reformulated or generalized as

$$C_{\theta} = \int \log_2 \left(1 + \frac{P_T h(\theta, \mathbf{f}_T, \mathbf{f}_R)}{\sigma_n^2} \right) p_{\theta}(\theta) d^n \theta, \quad (13)$$

where $\theta \in \mathbb{R}^n$ contains all unknown parameters with joint PDF $p_{\theta}(\theta)$, and $h(\cdot)$ is a channel power response with a specific realization of θ and the chosen beamforming vectors.

An important example scenario, in which the extended capacity in (13) can be utilized, is when the orientation of a user equipment (UE) is considered unknown. With traditional beam training procedures, the UE orientation can be neglected, but in the context of location-based geometric beamforming, the orientation must be always taken into account. However, it is possible to estimate the UE orientation jointly with the UE position, as shown, for example, in [14]. In addition, when

considering the beam training approach in Section III-B, the above-described capacity evaluation extension can be exploited to include beam training uncertainty with noisy measurements. Furthermore, by defining $h(\cdot)$ appropriately according to the underlying measurement model, the capacity with noisy beam training, can be obtained by replacing the integral in (9) with the extended capacity expression given in (13).

IV. NUMERICAL RESULTS AND ANALYSIS

In this section, we study and illustrate the proposed location-based beamforming approaches, without and with beam training by evaluating the achievable communications link capacity over a variety of considered system parameters. In order to evaluate the link capacities numerically, we fix the TX position as $\mathbf{x}_T = [0, 0]^T$, and for simplicity consider a LoS link with a free space path loss model. For the sake of presentation clarity, we consider beamforming only at the TX side by including a transmit antenna array of N elements with half-wavelength element spacing, and consequently fix the number of antenna elements in the RX as $M = 1$. It is worth noticing that in the considered LoS scenario, including the beamformer at the RX side would simply lead to an increased SNR at the RX. Moreover, in order to allow for different communications link budgets, we determine the transmit power as well as all the other parameters in the link budget so that the SNR at the considered 50 m distance without the beamforming gain results in three optional values of $\text{SNR}_{\text{ref}} \in \{0 \text{ dB}, 10 \text{ dB}, 30 \text{ dB}\}$, which could be considered as cell-edge, typical, and high-throughput scenarios.

The TX is considered to retain the RX position PDF, which is assumed to be normally distributed as $p_{\mathbf{x}}(\mathbf{x}) = \mathcal{N}(\boldsymbol{\mu}, \boldsymbol{\Sigma})$, where $\boldsymbol{\mu} \in \mathbb{R}^2$ is the mean vector and $\boldsymbol{\Sigma} \in \mathbb{R}^{2 \times 2}$ is the covariance matrix. For the numerical evaluations, we fix the RX position mean at 50 m distance from the TX and define $\boldsymbol{\mu} = [50, 0]^T$. Moreover, we assume the variances of the x-coordinate and y-coordinate to be equal and set $\boldsymbol{\Sigma} = \begin{bmatrix} \sigma^2 & \rho\sigma^2 \\ \rho\sigma^2 & \sigma^2 \end{bmatrix}$, where σ^2 describes the positioning error variance per coordinate dimension, and $\rho = 0.5$ is the assumed correlation between the x-coordinate and y-coordinate.

Regarding the location-based beamforming without beam training, we assume that the transmit beam is pointed towards the highest value of the RX position PDF. Regarding the evaluations with beam training, we assume a total set of N beams defined according to the columns of the discrete Fourier transform matrix, defined similarly as in [7]. It should be noticed that by this way one of the beams is always directly targeted to the maximum of the position PDF. Nevertheless, the utilization of the discrete Fourier transform based design automatically takes into account the angle-dependent angular resolution of the antenna array, as well as enables beam orthogonality when located exactly in the direction of any individual beam.

In Fig. 2, the cumulative distribution function of the channel capacity when purely location-based beamforming is considered, presented in (5), is shown with $\text{SNR}_{\text{ref}} = 10 \text{ dB}$ and $\sigma = 5 \text{ m}$ over different numbers of used transmit antenna elements N . It can be seen that when the number of used

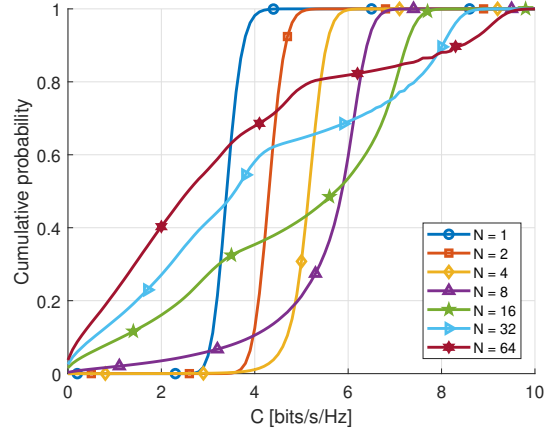


Fig. 2. Cumulative distribution of the radio link capacity without the beam training process, with $\text{SNR}_{\text{ref}} = 10 \text{ dB}$ and $\sigma = 5 \text{ m}$ for different numbers of transmit antenna elements N .

antenna elements is small (i.e., $N \leq 4$), the beamwidth is large and the RX is most likely located within the coverage of the main beam lobe, in which case the cumulative capacity is mostly affected by the location-dependent path loss $\zeta(\mathbf{x})$. However, when the number of used antenna elements is larger (i.e., $N \geq 8$), the beamwidth is significantly reduced and there is an increasing probability to partially or completely miss the RX, which consequently results in lower link capacities. Notably, in 50% of the realizations, a system with $N = 1$ provides larger capacity than a system with $N = 32$.

Considering the same beamforming strategy, the effect of the number of utilized antenna elements N (i.e., the beamwidth) on the expected capacity, as given in (6)-(7), is shown in Fig. 3 for different values of position error standard deviation (STD), σ , and the reference SNR, SNR_{ref} . In order to emphasize the connection between the number of used antenna elements and beamwidth, an additional x-axis considering the half-power beamwidth, defined as in [15], is added on top of the figure. As shown in Fig. 3, when the position error STD is $\sigma = 0.25 \text{ m}$, it is beneficial to use a high number of antenna elements, and thus, a narrow beamwidth. However, when increasing the positioning error to $\sigma = 1 \text{ m}$ or $\sigma = 5 \text{ m}$, the capacity is interestingly optimized for a specific beamwidth, that is, a specific number of used antenna elements. As seen in the figure, the optimal beamwidth with respect to capacity depends also on the underlying reference SNR value. This is one example of a concrete engineering and system optimization insight that the provided capacity expressions can provide. That is, there is a tradeoff between the beam-forming gain and the RX location uncertainty, that can be quantified through the derived capacity expressions thus allowing for beamformer optimization.

In Fig. 4, the channel capacity is shown for various numbers of used antenna elements as a function of position error STD with $\text{SNR}_{\text{ref}} = 10 \text{ dB}$. From the figure it is again evident that the communication link capacity can be optimized by choosing the number of used antenna elements (i.e. beamwidth) appropriately according to the level of the RX position uncertainty. Furthermore, similar to the well-known adaptive modulation and coding schemes, where the modulation order

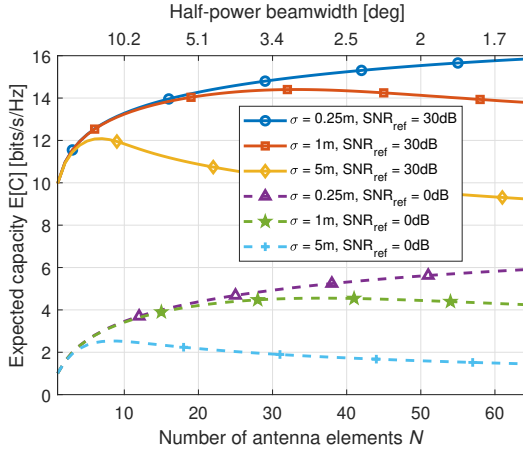


Fig. 3. Expected radio link capacity as a function of N without the beam training process for different values of position error STD and reference SNR.

and the channel coding rate are determined according to the observed SNR level, the beamwidth can be chosen based on the available positioning accuracy. It is also noted that in order to use the envisioned location-based beamforming efficiently with the highest considered number of antenna elements $N = 64$, sub-meter position accuracy is already needed in the considered scenario. Such positioning accuracy has been demonstrated feasible in recent works, e.g., [13], [14].

When introducing beam training, a narrow beam with a higher beam gain can be utilized even with uncertain RX position information, as discussed and analyzed in Section III-B. However, in this case the achieved beam gain becomes at the cost of training overhead, as defined in (12). To this end, in Fig. 5, the expected link capacity, is shown for different position error STDs and beam training overheads η as a function of the number of used training beams K with $\text{SNR}_{\text{ref}} = 10$ dB. In the case that accurate position information is available (i.e., $\sigma = 0.25$ m), the capacity degrades linearly, as the number of training beams is increased. On the other hand, when the position error STD is higher (i.e., $\sigma \geq 1$ m), an optimum number of training beams can again be found. Moreover, if the number of trained beams is smaller than the optimum value, expected capacity is decreased due to missing the target with the beamformer, whereas with too many training beams the capacity is lost for unnecessary training. In general, the provided capacity expressions allow for obtaining insight and optimizing the number of the training beams for the available positioning accuracy. We also note that since the total allowed time for the beam training is dependent on the channel coherence time, by defining a beam-wise channel utilization time it is also possible to obtain capacity limits for different mobility scenarios.

Finally, in order to illustrate the considered link capacity theorems under practical position PDF, we consider a 5G new radio (NR) network utilizing two separate frequency bands. The lower 3.5 GHz band is used to provide positioning information via an EKF-based solution to facilitate location-based beamforming at the higher 28 GHz mmWave band. Whereas the antenna array sizes at the lower 3.5 GHz band are

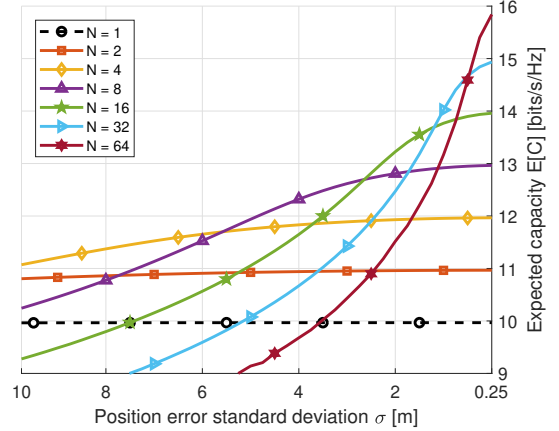


Fig. 4. Expected radio link capacity as a function of position error STD without the beam training process for different values of N .

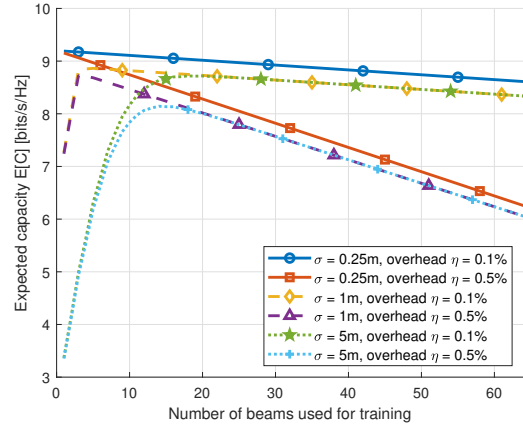


Fig. 5. Expected radio link capacity as a function of number of used training beams in the beam training process for different values of position error STD and training overhead η by using $N = 64$ transmit antenna elements.

assumed relatively small, considerably larger arrays, and thus narrower beams, are assumed at the mmWave band, where location-based beamforming can introduce several advantages. The considered system parameters are summarized in Table I.

The designed EKF-based solution seeks to sequentially estimate the position of a vehicle with a realistic polynomial acceleration profile in a similar manner as in [13]. The considered vehicle is moving with a varying speed of 15-45 km/h on top of the METIS Madrid grid environment [16], where an extensive ray-tracing [17] simulation is applied. The vehicle transmits a periodic uplink sounding reference signal (SRS) every 100 ms, which is received at LoS access nodes (AN) in known positions equipped with four arrays covering the whole azimuth-domain such that each array covers a 90-degree sector. In particular, the beamformers at the active ANs are directed towards the a priori estimate of the UE given by the positioning EKF employing only time of arrival estimates from five closest LoS-ANs in a similar two-fold estimation process as proposed originally in [13].

At each considered 100 ms time interval, the mmWave beam is directed towards the position estimate provided by

TABLE I
POSITIONING AND CAPACITY EVALUATION PARAMETERS

Parameter	Positioning	Capacity evaluation
Carrier frequency	3.5 GHz	28 GHz
Bandwidth	50 MHz	100 MHz
Subcarrier spacing	15 kHz	60 kHz
UE antenna	1 dipole element	1 dipole element
AN antenna	4×4 URA (3GPP patch)	Varying N×N URA (3GPP patch)
Evaluation time interval	100 ms	100 ms
Number of used closest LoS-ANs	5	1
UE speed	15-45 km/h	15-45 km/h

the cmWave EKF. After this, the mmWave link capacity is evaluated subcarrier-wise for different considered AN array sizes, and the overall capacity is defined as a sum of capacities over all active subcarriers. Cumulative distributions for the obtained overall mmWave link capacities, considering different uniform rectangle array (URA) antenna sizes at the AN, are shown in Fig. 6. Despite the varying system geometry due to vehicle mobility, the introduced realistic multipath propagation, and the PDF linearization errors due to the EKF, the presented cumulative distributions are strongly resembling the cumulative distributions of the pure LoS scenario with static environment, shown earlier in Fig. 2. Based on Fig. 6, it is clear that the chosen array size, and thus the beamwidth, has a significant influence on the link capacity, with similar insight as in the earlier examples. Whereas the largest considered array of size 64×64 is able to provide the maximum instantaneous capacity, the smaller array sizes can provide more limited capacity but in more consistent manner. In the considered scenario, the best average capacity of 1.56 Gbit/s is provided by the 16×16 array.

V. CONCLUSION

In this paper, we studied the capacity of a beamformed radio link utilizing location-based beamforming based on available position information, given as an arbitrary position PDF. By considering both the purely location-based beamformer and the location-aided beam training based beamformer, capacity expressions were formulated and derived. The capacity expressions were then evaluated numerically in selected scenarios while varying many of the basic system parameters. In addition, a practical 5G NR deployment scenario with realistic ray-tracing-based multipath propagation was studied and demonstrated, with an EKF-based positioning solution at the 3.5 GHz band to facilitate location-based beamforming at the 28 GHz band. The presented results show that the wireless link capacity can be optimized, for example, with respect to the number of used antenna array elements, which define the array beamwidth, or with respect to the number of used training beams if explicit beam-sweeping based training procedure is incorporated. Depending on the accuracy of the available position estimates, it was shown that the optimal antenna array size as well the amount of training beams, in the training based system, vary. Overall, the proposed approach allows for maximizing the radio link capacity under any given positioning uncertainty while at the same time providing means to optimize the use of the radio resources

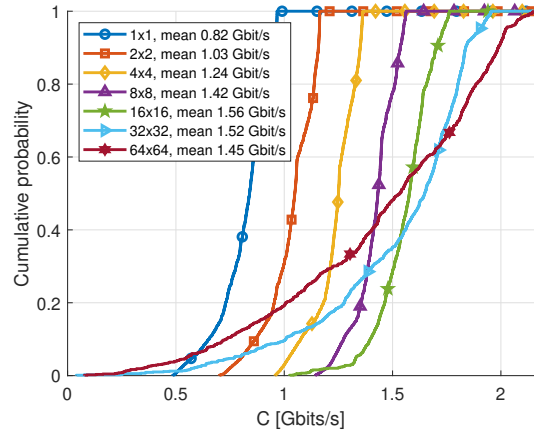


Fig. 6. Cumulative distribution of mmWave radio link capacity at Madrid map with the EKF-based cmWave positioning in realistic ray-tracing simulation for different sizes of transmit antenna array. Additional multimedia material is available related to the EKF-based tracking feeding the mmWave beamformer.

and array configuration. Our future work focuses on extending the analysis to more complicated NLoS propagation scenarios.

REFERENCES

- [1] A. V. Lopez *et al.*, "Opportunities and Challenges of mmWave NR," *IEEE Wireless Commun.*, vol. 26, no. 2, pp. 4–6, April 2019.
- [2] K. Huang and Z. Wang, *Millimeter Wave Communication Systems*, ser. IEEE Series on Digital & Mobile Communication. Wiley, 2011.
- [3] K. David and H. Berndt, "6G Vision and Requirements: Is There Any Need for Beyond 5G?" *IEEE Veh. Technol. Mag.*, vol. 13, no. 3, pp. 72–80, Sep. 2018.
- [4] M. Giordani *et al.*, "A Tutorial on Beam Management for 3GPP NR at mmWave Frequencies," *IEEE Commun. Surveys Tutorials*, vol. 21, no. 1, pp. 173–196, Firstquarter 2019.
- [5] C. Liu *et al.*, "Millimeter-Wave Small Cells: Base Station Discovery, Beam Alignment, and System Design Challenges," *IEEE Wireless Commun.*, vol. 25, no. 4, pp. 40–46, AUGUST 2018.
- [6] D. De Donno, J. Palacios, and J. Widmer, "Millimeter-Wave Beam Training Acceleration Through Low-Complexity Hybrid Transceivers," *IEEE Transactions on Wireless Communications*, vol. 16, no. 6, pp. 3646–3660, June 2017.
- [7] G. Destino and H. Wymeersch, "On the trade-off between positioning and data rate for mm-wave communication," in *Proc. 2017 IEEE ICC Workshops*, May 2017, pp. 797–802.
- [8] J. Choi, "Beam Selection in mm-Wave Multiuser MIMO Systems Using Compressive Sensing," *IEEE Trans. Commun.*, vol. 63, no. 8, pp. 2936–2947, Aug 2015.
- [9] P. Kela *et al.*, "Location Based Beamforming in 5G Ultra-Dense Networks," in *Proc. IEEE 84th VTC-Fall*, Sept. 2016, pp. 1–7.
- [10] Y. Cui *et al.*, "Optimal nonuniform steady mmwave beamforming for high-speed railway," *IEEE Trans. Veh. Technol.*, vol. 67, no. 5, pp. 4350–4358, May 2018.
- [11] J. Talvitie *et al.*, "Positioning and Location-Based Beamforming for High Speed Trains in 5G NR Networks," in *2018 IEEE Globecom Workshops*, Dec. 2018, pp. 1–7.
- [12] G. Destino *et al.*, "Impact of imperfect beam alignment on the re-positioning trade-off," in *Proc. 2018 IEEE WCNC*, April 2018, pp. 1–5.
- [13] M. Koivisto *et al.*, "Joint Device Positioning and Clock Synchronization in 5G Ultra-Dense Networks," *IEEE Trans. Wireless Commun.*, vol. 16, no. 5, pp. 2866–2881, May 2017.
- [14] J. Talvitie *et al.*, "High-Accuracy Joint Position and Orientation Estimation in Sparse 5G mmWave channel," in *Proc. IEEE ICC*, May 2019.
- [15] M. Plotkin, "Beamwidth of phased arrays," *IEEE Trans. Antennas Propag.*, vol. 21, no. 5, pp. 695–697, Sep. 1973.
- [16] METIS, "D6.1 Simulation guidelines," Oct. 2013.
- [17] 3GPP TR 38.901, "Study on channel model for frequencies from 0.5 to 100 GHz," 2020.